

Molecular dynamics study of the cations, water molecules, and polymer chains in Nafion type membranes

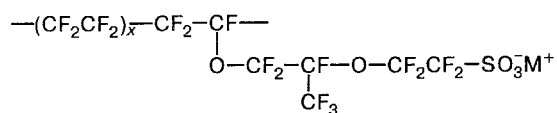
Yu. A. Dyakov and Yu. K. Tovbin*

L. Ya. Karpov Institute of Physical Chemistry,
10 ul. Vorontsovo Pole, 103064 Moscow, Russian Federation.
Fax: +7 (095) 975 2450

The structure and dynamics of the hydrated cationic complexes in Nafion type membrane pores has been studied by the molecular dynamics approach. The mechanism of the cationic transport has been examined. The dependence of the cationic transport coefficients on temperature and the number of water molecules has been investigated.

Key words: molecular dynamics, potential, cation, Nafion, membrane.

Membrane of the Nafion type refers to an amorphous polymeric substance with a monomeric unit of the following structure



where M^+ is alkali metal cation, H^+ or NH_4^+ . These membranes are known to be selective for different types of cations and are used for separation of ionic mixtures, in particular for industrial preparation of sodium hydroxide and chlorine. At the micro level the membrane has a bilayer structure¹ that consists of slit-like pores with hydrated ions inside and fluorine-ethylene interlayering (Fig. 1). The pore has two layers of side branches with terminal SO_3^-M^+ ionogenic groups. In the presence of water these terminal groups dissociate forming the hydrated complexes $\text{M}^+(\text{H}_2\text{O})_m$, where m is the number of water molecules in the hydrate shell of alkali metal. The ionic transport of Nafion type membranes was experimentally established to be of threshold character and depends on the moisture content n (the number of water

molecules per SO_3^- group), the ionic transport occurring at different n -values with different kinds of cations. It is suggested that the transport takes place when the hydrate shells of the neighboring ionogenic groups are overlapped.

Using the molecular dynamics² (MD) method we have investigated the mechanism of cation transport in the Nafion type membrane and the dependence of the cation transport coefficients on temperature and the moisture content n . The microstructure and the dynamics of the hydrate complexes of cations were analyzed using the membrane with SO_3^-M^+ ionogenic groups as an example.

Model description. The calculations were made inside a parallelepiped cell with a base of quadrate form (17.82×17.82 Å); the height was changed in the range from 32 to 40 Å depending on the moisture content. The choice of geometric dimensions of the cell was based on the data of X-ray analysis and Mössbauer spectroscopy¹. There were 8 polymer chains in the cell (4 at the top and 4 at the bottom). The internal space between the chains was filled with water molecules, the number (n) of which varied from 6 to 12. Water molecules were represented as a three-point-model³ with charges centered at the oxygen and hydrogen atoms and the H—O—H bond angle equal to 104.5° . The oxygen atom had a charge of $-0.68e$; the hydrogen one — of $+0.34e$. The Li ion was considered as a mobile particle with a charge of $+e$; the side chain had a total negative charge of $-e$. The charge distribution for the side chain atoms was found by the quantum-chemical MNDO method. For simplicity of the calculations the CF_2 and CF_3 groups were replaced by the effective atoms with empirically selected radii and potential parameters corresponding to those of the fluorine atom. The charges of the effective atoms were equal to the sum of the charges of their constituent atoms. Fluorine atoms covering the walls of the pore were replaced by a unified electrically neutral plane with

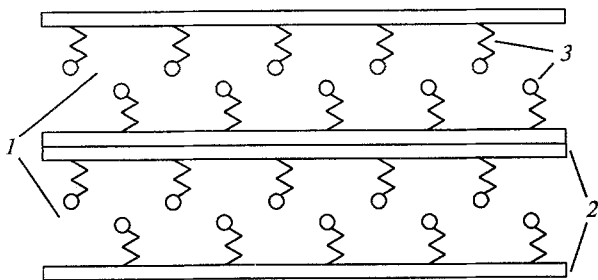


Fig. 1. Membrane's microstructure: 1, membrane pore; 2, polymer interlayer between the pores; 3, polymer side chains with SO_3^-M^+ terminal groups.

potential parameters of fluorine atoms. The interaction between the system's atoms and the pore wall was described by the potential

$$U(r) = -\frac{A}{r^3} + \frac{B}{r^9} \quad (1)$$

The potential of the atoms' interaction was defined as the sum of the Coulomb's and Lennard-Jones's potentials:

$$U(r) = U_c(r) + U_{LJ}(r),$$

$$U_c(r) = \frac{q_1 q_2}{r}, \quad U_{LJ}(r) = -\frac{A}{r^6} + \frac{B}{r^{12}} \quad (2)$$

where q_1 and q_2 are the charges of atoms, A and B are the potential parameters, r is the distance between atoms. The interaction between O and H atoms of the water molecules was described by the potential³:

$$U_{LJ}(r) = -\frac{A}{r^6} + \frac{B}{r^{12}} \quad (3)$$

The potential parameters used in the calculations are given in Table 1.

The calculation followed the Runge-Kutt fourth order algorithm. The integration step was chosen to be equal to $1.5 \cdot 10^{-15}$ s. The number of the steps was of ~60000. The periodic boundary conditions along the x and y axes were used in the calculation. Basic calculations were performed for the immobile polymer chains. The values of the Lennard-Jones potential were taken to be equal 0, beginning with the distance equal to the half

of the cell's length $L/2$. For simplicity of the calculations the potential of the interaction of every atom with other immobile atoms was divided into two parts:

$$U(r) = U_1(r) + U_2(r)$$

$$U_1(r) = \begin{cases} \frac{A}{r^n} + \frac{nA}{3} \frac{r^3}{r_c^{n+3}} - \frac{n+3}{3} \frac{A}{r_c^n}, & r \leq r_c \\ 0, & r > r_c \end{cases} \quad (4)$$

$$U_2(r) = \begin{cases} -\frac{nA}{3} \frac{r^3}{r_c^{n+3}} + \frac{n+3}{3} \frac{A}{r_c^n}, & r \leq r_c \\ \frac{A}{r^n}, & r > r_c \end{cases}$$

The first part involves the interaction potentials for the atoms of $r < 4.5$ Å distant from each other. The second part involves the interaction potentials for the atoms separated by from each other by distance $r > 4.5$ Å. It was decided to present the second part of the potential as a three-dimensional grid and to calculate this part before the beginning of the main program calculation. During the MD-program execution the values of this part of the potential in any point of the cell were calculated from its values at grid nodes using splines⁷. The final potential was found during the program calculation as the sum of the both parts of the potential.

Table 1. Lennard-Jones parameter and the charges of chain atoms, water molecules and lithium cations

| Atom | q/e | Water | | | | Li | |
|-------------------|---------|---------|---------|---------|--------|---------|----------|
| | | $-A_O$ | B_O | $-A_H$ | B_H | $-A$ | B |
| O | — | 282.00 | 283000 | 126.30 | 27310 | 22.836 | 10028.8 |
| CF | -0.2198 | 1212.84 | 3993016 | 737.87 | 711288 | 114.940 | 193813.6 |
| CF ₃ | 0.5579 | 1212.84 | 3993016 | 737.87 | 711288 | 114.940 | 193813.6 |
| CF ₂ | -0.2041 | 1212.84 | 3993016 | 737.87 | 711288 | 114.940 | 193813.6 |
| O | -0.4190 | 282.00 | 283000 | 126.30 | 27310 | 22.836 | 10028.8 |
| CF ₂ | 0.1297 | 1212.84 | 3993016 | 737.87 | 711288 | 114.940 | 193813.6 |
| CF ₂ | -0.3666 | 1212.84 | 3993016 | 737.87 | 711288 | 114.940 | 193813.6 |
| S | 1.6304 | 745.61 | 1784000 | 420.73 | 273400 | 67.968 | 80094.6 |
| O | -0.7002 | 282.00 | 283000 | 126.30 | 27310 | 22.836 | 10028.8 |
| O | -0.7116 | 282.00 | 283000 | 126.30 | 27310 | 22.836 | 10028.8 |
| O | -0.6966 | 282.00 | 283000 | 126.30 | 27310 | 22.836 | 10028.8 |
| Li | 1.000 | 470.00 | 19200 | 167.00 | 3000 | 25.300 | 4483.2 |
| O | -0.6800 | 200.00 | 410000 | 3760.00 | 9700 | 470.00 | 19200 |
| H | 0.3400 | 3760.00 | 9700 | 40.00 | 3800 | 167.00 | 3000 |
| F _(cr) | — | 105.69 | 16790 | 49.839 | 1797.1 | 118.79 | 14675.76 |

Note. Interaction potential is used in the form of $U_{ij} = \frac{A_{ij}}{R_{ij}^6} + \frac{B_{ij}}{R_{ij}^{12}} + \frac{C_{ij} q_1 q_2}{R_{ij}}$,

where A_{ij} (kcal Å⁶ mol⁻¹), B_{ij} (kcal Å¹² mol⁻¹), and $C_{ij} \cdot 332.156$ (kcal Å² (e²·mol)⁻¹) are constants, R_{ij} (Å) are distances between atoms, q_i/e are charges of atoms; the last line gives the parameters of interaction between atoms and wall.

Results and Discussion

The distribution of water molecules in the membrane pore, the structure of Li hydrate complexes and the membrane ionic permeability were investigated as a function of its moisture content and the temperature. From the analysis of the cell instant photographs at moisture content $n = 6, 8, 10$ and 12 at the temperature of 360 K it appears that at $n = 6$ and 8 the water distribution has a striated character with the density maxima near sulfo groups. Li cations are arranged in the boundary area of the pore. At $n = 10$ and 12 the water molecules are displaced into the central area of the pore and the unified hydrate layer is formed. When cations arrive into this layer they lose the connection with their sulfo group and move relatively free along the pore of the membrane. At a time a minor amount of cations is located at the central area of the pore. Main part of cations is situated near sulpho groups and doesn't take part in the cation transport. It explains the fact that the coefficient of cations diffusion in the membrane is significantly lower than the corresponding value of an infinitely diluted electrolyte. The dependence of the coefficient of Li cations diffusion on the moisture content is shown on Fig. 2.

To test the validity of the approximation of the immobile side chains a more precise calculation for the mobile side chains was performed. In this case the curve of the membrane cation transport was shifted by unity to smaller values of n , but it didn't change qualitatively the results obtained. Curve shift results from the exclusion of water molecules from interchain space into central area of the pore. These results correlate with the experimental data.^{8,9}

The temperature function of the diffusion coefficients for cations (Fig. 3) and water (Fig. 4) in the membrane pore at the moisture content $n = 12$ was studied. It emerges that at the temperature $T < 270$ K the cation transport is virtually absent in the pore. In the same range of temperature the mean-square displacement of water molecules depends almost linearly on time suggesting a normal diffusion. At $T > 270$ K cations

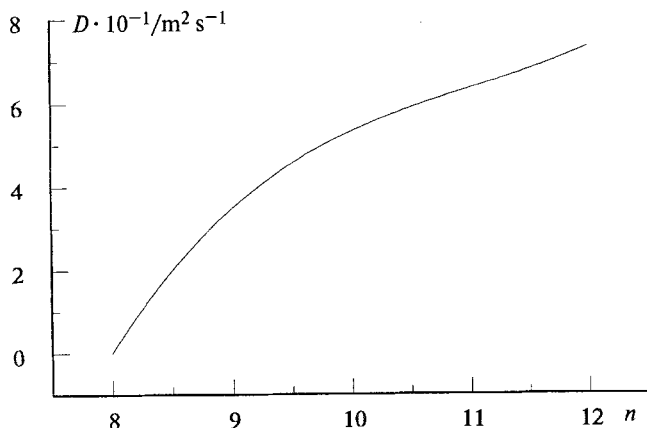


Fig. 2. Dependence of Li diffusion coefficient on the moisture content ($T = 390$ K).

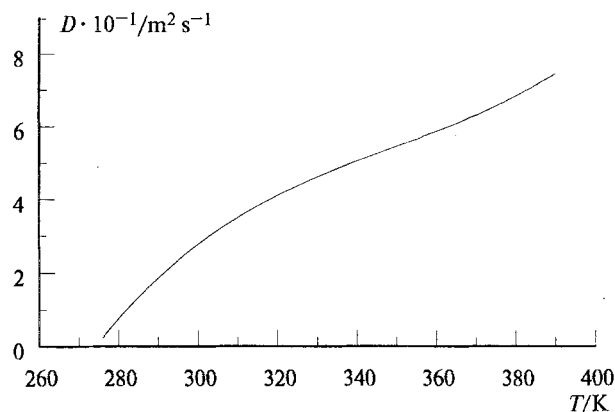


Fig. 3. Temperature dependence of Li diffusion coefficient ($n = 12$).

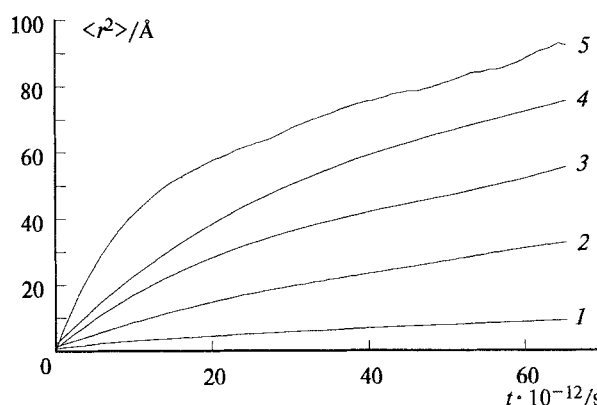


Fig. 4. Mean-square displacement of water molecules at the temperatures T/K : 228 (1), 276 (2), 302 (3), 322 (4), 390 (5).

ions begin to move and the time dependence of the mean-square displacement of water molecules becomes nonlinear. This fact appears to be associated with freezing out of translation motion of cations and the collective movement of the water molecules incorporated in hydrate shells of the cations. As it was shown by ESR and NMR¹⁰ methods, the increase of the coefficient of the water translation diffusion in membrane is observed in the range of 270 – 290 K. This fact is consistent with the results obtained by the MD method.

For the purpose of investigation of the structure of hydrated cationic complexes in the membrane pore we plotted the graphs of the radial distribution function of $\text{Li}^+ - \text{O}(\text{H}_2\text{O})$ (Fig. 5) and $\text{O}(\text{H}_2\text{O}) - \text{O}(\text{H}_2\text{O})$ (Fig. 6), where H_2O is the water incorporated in the cations hydrate shells, and the graph of the angular distribution function of $\text{O} - \text{Li} - \text{O}$, where O is the oxygen of the water molecules incorporated in the first coordination sphere of Li hydrate shell. The first peak of the radial distribution function is located at 1.98 Å distance that agree with the well-known X-ray analysis data for Li-containing solutions of electrolytes. Maxima of the angular distribution function $\text{O} - \text{Li} - \text{O}$ are located at 90° and 180° that correlates with the octahedral structure of Li hydrate shell. Maxima of the distribution function

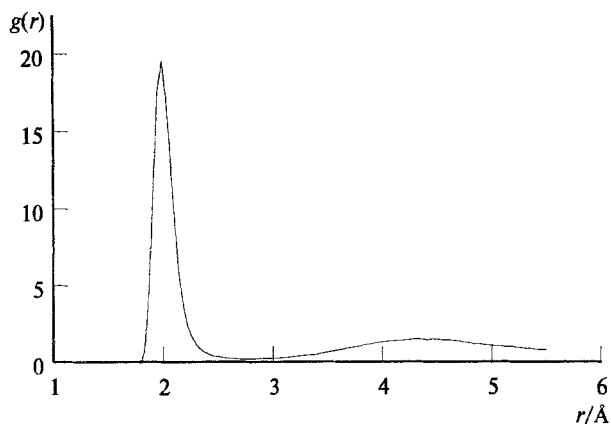


Fig. 5. Radial distribution function Li—O, where O is the oxygen of water molecules incorporated in Li hydrate shell.

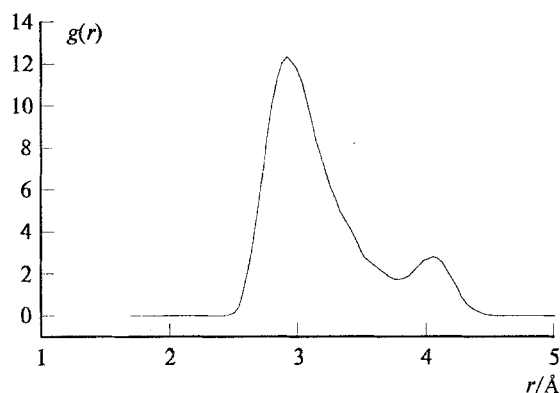


Fig. 6. Radial distribution function O—O, where O is the oxygen of water molecules incorporated in Li hydrate shell.

O(H₂O)—O(H₂O) are located at 2.8 and 4.0 Å distances that also correlates with the octahedral structure of the hydrate shell. Analysis of the particles tracks showed that the average number of the water molecules incorporated in Li hydrate shell falls in the range from 3 to 4, i.e., some vertices of the octahedron are free. Fig. 7 demonstrates the logarithmic time dependence of the number of water molecules incorporated initially in the first correlation sphere of Li hydrate complex and left there to the instant of time t . The dependence is linear, which let us calculate the energy of the elimination of the water molecule from the lithium hydrate shell. It is equal to 3.8 Kcal mol⁻¹. This value is significantly greater than kT that argues for the stability of the hydrate complex.

Cation transport of the Nafion type membrane has an volume nature and is achieved in presence of a central hydrate layer in the membrane pore. At low moisture content this layer is distorted and the water is congregated in the boundary areas that make cation transport difficult. Cation transport in the membrane is absent at temperatures $T < 270$ K. Fixing the position of side chains used for the simplicity of the calculations results in shifting the cation transport threshold of the

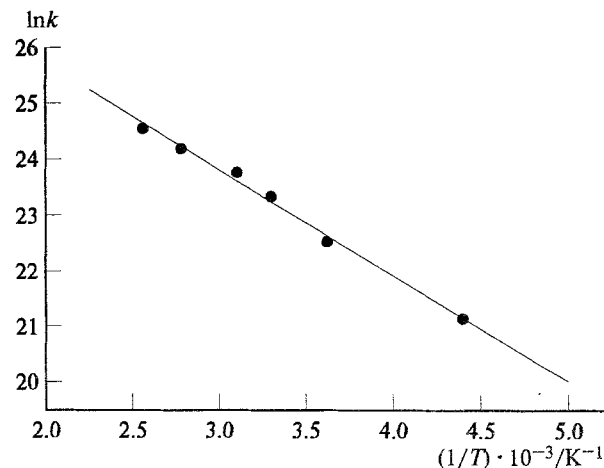


Fig. 7. Rate constant of water exchange in Li hydrate shell.

membrane to lower n values. In the comparison of the MD-results with the experimental data, consideration must be given to this admission. Li hydrate complex has the octahedral structure with average number of water molecules equal to 4. The energy of the elimination of the water molecule from the lithium hydrate shell is equal to 3.8 kcal · mol⁻¹ that argues for the stability of the hydrate complex.

The present work was made possible in part by financial support of the International Science Foundation (Grant MPG000) and the Russian Foundation for Basic Research (Grant 93-03-4205).

References

1. S. F. Timashev, *Fiziko-khimiya membrannykh processov* [Physics and chemistry of membrane processes], Khimiya, Moscow, 1988, 238 p (in Russian).
2. M. P. Allen and D. J. Tildesley, *Computer Simulation of Liquids*, Oxford Univer. Press, 1987.
3. G. G. Malenkov, M. M. Frank-Kamenetsky, and A. G. Grivtsov, *Zhurn. struktur. khimii*, 1987, **28**, 81 [*J. Struct. Chem. USSR*, 1987, **28** (Engl. Transl.)].
4. N. F. Vasyutkin and Yu. K. Tovbin, *Vysokomolekularnye soedinenia*, 1993, **53**, A, 1600 [*Polim. Sci.*, 1993, **53**, A (Engl. Transl.)].
5. Yu. K. Tovbin, Yu. A. Dyakov, and N. F. Vasyutkin, *Zhurn. phys. khimii*, 1993, **67**, 2122 [*Russ. J. Phys. Chem.*, 1993, **67** (Engl. Transl.)].
6. N. F. Vasyutkin, I. K. Vorontsova, I. D. Miheikin, and Yu. K. Tovbin, *Zhurn. phys. khimii*, 1992, **66**, 1302 [*Russ. J. Phys. Chem.*, 1992, **66** (Engl. Transl.)].
7. V. S. Ladygin, *Preprint of IPM M.V. Keldish AN SSSR*, 1991, No. 25 (in Russian).
8. V. I. Volkov, S. N. Gladkikh, and S. F. Timashev, *Khim. fizika* [Chem. Physics], 1983, **2**, 49 (in Russian).
9. I. A. Nesterov, V. I. Volkov, K. K. Puhov, S. F. Timashev, *Khim. fizika* [Chem. Physics], 1990, **9**, 1155 (in Russian).
10. N. Ya. Steinschneider, *Zhurn. phys. khimii*, 1995, **69** [*Russ. J. Phys. Chem.*, 1995, **69** (Engl. Transl.)].

Received December 7, 1994